Molecular Vision 2015; 21:688-698 <http://www.molvis.org/molvis/v21/688>
Received 8 March 2015 | Accepted 10 June 2015 | Published 12 June 2015

Fasudil hydrochloride, a potent ROCK inhibitor, inhibits corneal neovascularization after alkali burns in mice

Peng Zeng,[1] Rong-biao Pi,[2] Peng Li,[3] Rong-xin Chen,[1] Li-mian Lin,[1] Hong He,[4] Shi-you Zhou[1]

(The first three of the authors contributed equally to this work.)

[1]Zhongshan Ophthalmic Center of Sun Yat-sen University, The State Key Laboratory of Ophthalmology,Guangzhou, China; [2]Department of Pharmacology & Toxicology, School of Pharmaceutical Sciences, Sun Yat-Sen University, Guangzhou, China; [3]Department of Ophthalmology, No.181 Hospital of PLA, Guangxi, Guilin, China; [4]Hainan Eye Hospital of Zhongshan Ophthalmic Center, Haikou, Hainan Province, China

Purpose: To investigate the effects and mechanisms of fasudil hydrochloride (fasudil) on and in alkali burn-induced corneal neovascularization (CNV) in mice.

Methods: To observe the effect of fasudil, mice with alkali-burned corneas were treated with either fasudil eye drops or phosphate-buffered saline (PBS) four times per day for 14 consecutive days. After injury, CNV and corneal epithelial defects were measured. The production of reactive oxygen species (ROS) and heme oxygenase-1(HO-1) was measured. The infiltration of polymorphonuclear neutrophils (PMNs) and the mRNA expressions of CNV-related genes were analyzed on day 14.

Results: The incidence of CNV was significantly lower after treatment with 100 μM and 300 μM fasudil than with PBS, especially with 100 μM fasudil. Meanwhile, the incidences of corneal epithelial defects was lower (n=15, all $p<0.01$). After treatment with 100 μM fasudil, the intensity of DHE fluorescence was reduced in the corneal epithelium and stroma than with PBS treatment (n=5, all $p<0.01$), and the number of filtrated PMNs decreased. There were significant differences between the expressions of VEGF, TNF-a, MMP-8, and MMP-9 in the 100 μM fasudil group and the PBS group (n=8, all $p<0.05$). The production of HO-1 protein in the 100 μM fasudil group was 1.52±0.34 times more than in the PBS group (n=5 sample, $p<0.05$).

Conclusions: 100 μM fasudil eye drops administered four times daily can significantly inhibit alkali burn-induced CNV and promote the healing of corneal epithelial defects in mice. These effects are attributed to a decrease in inflammatory cell infiltration, reduction of ROS, and upregulation of HO-1 protein after fasudil treatment.

Commonly associated with inflammatory, infectious, and traumatic disorders of the ocular surface, corneal neovascularization (CNV) is a severe sight-threatening condition. When the effect of angiogenic factors overcome that of antiangiogenic factors in corneal burns, corneal neovascularization will be brought out [1-3]. According to current understanding, inflammatory cytokines and reactive oxygen species (ROS) are two of the major angiogenic factors in the development of CNV after injury.

The current agents for inhibiting CNV includes anti-angiogenic factors [4,5], anti-inflammatory agents [6,7], agents for anti-remodeling of the extracellular matrix [8,9], and agents for anti-oxidative stress [10]. As a potential regulator of cellular ROS metabolism, the small GTPase RhoA and its downstream effector ROCK in the RhoA/ROCK signal pathway has recently been shown to play a critical role in angiogenesis [11,12]. ROCK inhibitors could protect endothelial cells from inflammatory damage by suppressing nuclear factor kappa B signaling [13,14] and reducing ROS production [15]. As a potent inhibitor of Rho-kinase, fasudil has an inhibitory effect similar to ATP [16]. In this study, fasudil was demonstrated to inhibit alkali burn-induced CNV not only by decreasing inflammation but also by reducing ROS via the RhoA/ROCK pathway and by increasing the heme oxygenase-1 (HO-1) protein, a protective factor against ROS.

Correspondence to: Shi-you Zhou, #54 south Xianlie Road,The State Key Laboratory of Ophthalmology, Zhongshan Ophthalmic Center of Sun Yat-sen University, Guangzhou, China 510060; Phone: 8620-87331550, FAX: 8620-87331550; email: zhoushiy@mail.sysu.edu.cn

METHODS

Animals: Female BALB/c mice aged 4 to 6 weeks and weighting between 16 and 20 g were purchased from the Guangdong Provincial Center for Animal Research in Guangzhou, China. The right eye of each mouse was selected for experimentation. All experiments on animals were conducted in accordance with the ARVO Statement for the Use of Animals in Ophthalmic and Vision Research. The research protocol was approved by the Animal Care Committee of the

Zhongshan Ophthalmic Center at Sun Yat-sen University in China.

Alkali burn- induced CNV: CNV was induced by alkali burns using a method outlined in previous reports [17]. In brief, after the mice were sedated with an intraperitoneal injection of general anesthesia consisting of 4.3% chloral hydrate [10 ml/kg] and a topical anesthesia consisting of a drop of 0.5% proparacaine hydrochloride (Alcaine eye drops, Alcon Inc., Fort Worth, TX), a 2 mm diameter filter paper soaked with 2 µl of 0.1 M NaOH solution was placed on the central cornea for 40 s, followed by immediate rinsing with 30 ml of 0.9% saline solution for 10 s. The entire corneal limbus and epithelium were then scraped off with a surgical blade under a microscope. Tobramycin ophthalmic ointment (Tobrex, Alcon Inc.) was administered after the operation.

Treatment with fasudil hydrochloride eye drops: The fasudil hydrochloride (Asahi Kasei Inc., Tokyo, Japan) was diluted in phosphate-buffered saline (PBS) to make different concentrations of fasudil eye drops. To observe the antiangiogenic effects of fasudil, 75 mice with alkali burns were randomly assigned to either the experimental groups to be treated topically with 30, 100, 300, and 1000 µM fasudil eye drops or to the control groups to be treated with PBS eye drops four times daily for 14 consecutive days (n=15 in each group). All the mice were killed on day 14 for immunohistopathological examination and reverse quantitative real-time polymerase chain reaction (PCR) analysis.

To detect the production of HO-1 in the murine corneas, another 50 mice with alkali burns were randomly treated with 100 µM fasudil eye drops or PBS eye drops four times daily for 4 consecutive days (n=25 in each group). To detect the production of ROS, 15 mice with alkali burns were randomly assigned to be treated with 100 µM fasudil eye drops, PBS eye drops, or nothing every 2 h for six consecutive hours (n=5 in each group), while another five normal mice without burns were assigned to a control group. The murine corneas were then procured for the analysis of ROS production.

Quantification of CNV and measurement of corneal epithelial defects: On days 4, 7, 10, and 14 after receiving alkali burns, the murine corneas were examined and photographed with a digital camera (Cannon, Tokyo, Japan) attached to a slit-lamp microscope (SL-120, Zeiss Inc., Jena, Germany). After the cycloplegia with a tropicamide eye drop (Wujing Pharmaceutical Company, Wuhan, China), CNV was observed under a white light. Corneal epithelial defects were then revealed using 0.5% fluorescein staining and were observed under a cobalt blue light. Three consecutive photos with satisfactory full-face imaging were used for image analysis. Image J software (ver. 1.62) was downloaded from the US National Institutes of Health (NIH) website and used for quantitative analysis, as documented in a previous report [18]. The consecutive photos of each mouse were used to measure the areas of CNV, epithelial defects, and the entire cornea, and then their percentages were calculated.

Measurement of ROS: Six hours after the alkali burn, the murine eyeballs were enucleated and immediately frozen in optimum cutting temperature (OCT) compound (Sakura Finetek, Torrance, CA). The cryopreserved blocks were cut until the first slide with corneal tissue was observed. The next five 30th slides of 10 µm thickness were then collected for immunostaining. when the first slide was observed, then the last section of every 30 consecutive cuts was procured to get five sections. Each section was 10 µm thickness.Unfixed cryosections were incubated with 5 µM dihydroethidium (DHE, ROS Fluorescent Probe, Eugene, OR) for 15 min at 37 °C, as previously reported [19]. The negative control was created by incubating sections with PBS instead of DHE. Sections were examined using a fluorescence microscope at 400× magnification (Olympus IX51, Tokyo, Japan) and photographed with an exposure time of 695 ms. The intensity of fluorescein staining was measured in the corneal epithelium and stroma using Image J 1.62 software.

Immunohistochemistry: Fourteen days after the alkali burns, seven mice in each of the 100 µM and PBS groups were randomly killed and their eyeballs were enucleated for immunohistochemistry. The eyeballs were fixed in a 10% neutral buffered formaldehyde solution and embedded in paraffin. The paraffin blocks containing the samples were cut until the first slide with corneal tissue was observed. Then the next three 20th slides of 5 µm thickness were collected for immunostaining, and another three 25th slides were collected for hematoxylin-eosin (H-E) staining. When the first slide was observed, then the 20th and 25th sections of every 30 consecutive cuts was procured to get three sections each for immunostaining and HE staining. For the immunostaining of polymorphonuclear neutrophils (PMNs), sections were deparaffinized and boiled in antigen retrieval solution (Dako, Glostrup, Denmark) for 15 min. Nonspecific staining was blocked with 1% bovine serum albumin (BSA; Sigma-Aldrich, St. Louis, MO) for 1 h at room temperature. Sections were then incubated with the primary antibody (monoclonal rat antibody against mouse neutrophil marker NIMP-R14; sc59338, Santa Cruz Biotechnology, Santa Cruz, CA) diluted with 1% BSA (1:300) overnight at 4 °C. After three washes with PBS for 15 min, sections were incubated with HRP-conjugated secondary anti-rat IgG antibody (ZSGB-BIO Institute of Biotechnology, Beijing, China) for 1 h at room temperature and then washed again with PBS. The negative control was

Table 1. Primer sets for real-time PCR.

Gene	Forward (5′-3′)	Reverse (5′-3′)
GAPDH	GTTGTCTCCTGCGACTTCA	TGGTCCAGGGTTTCTTACT
VEGF	ACTATTCAGCGGACTCACC	AACCAACCTCCTCAAACC
VEGFR1	ACCCTGGTAAAGCAACTAA	GCACGGAGGTGTTGAAAG
VEGFR2	TGTGAACGCTTGCCTTAT	CAACATCTTGACGGCTACT
TNF-α	TCAGAATGAGGCTGGATAA	AAGAGGAGGCAACAAGGT
IL-1β	CTCCATGAGCTTTGTACAAGG	TGCTGATGTACCAGTTGGGG
MMP-2	CCCCGATGCTGATACTGA	CACTGTCCGCCAAATAAA
MMP-8	GATTATGGAAATGCCTCG	CTTCAGCCCTTGACAGC
MMP-9	CAGCCAACTATGACCAGGAT	CTGCCACCAGGAACAGG

created by incubating sections with PBS instead of the primary antibody. The sections were then counterstained with Hoechst 33342 for 2 min. The sections were then washed three times in PBS for 3 min before being mounted on glass slides. The corneal sections were procured for histopathological study, just as in the procedures for immunostaining, and the slides were deparaffinized and regularly stained with H-E. Corneal morphology and the infiltrated PMNs in the corneal stroma were visualized and photographed with a fluorescence microscope (Olympus IX51). The number of infiltrated inflammatory cells in the cornea, including PMNs, was counted in five randomly selected fields (at 400× magnification) of a slide.

Analysis of mRNA expression: Real-time quantitative reverse transcription PCR (real-time qRT-PCR) was performed to detect the mRNA expression levels of the VEGF, VEGFR1, VEGFR2, TNF-α, IL-1β, MMP-2, MMP-8, and MMP-9 genes in the murine corneas. On day 14 after the burns, 8 mice from each of the 100μM group and the PBS group were euthanized by cervical dislocation, and their right corneas were procured. The total RNAs of each cornea were immediately isolated using an RNeasy Micro Kit (Qiagen, Valencia, CA). After quantification of the RNA concentration, the total RNAs were treated with DNase I (Sigma-Aldrich) to remove any contaminated genomic DNA. A total of 0.5 μg RNA was reverse transcribed into cDNA in a 20 μl volume reaction system using a Maxima First Strand cDNA Synthesis Kit (Fermentas International Inc., Burlington, ON, Canada). Samples of synthesized cDNA were divided into aliquots and stored at -80 °C.

Real-time qRT-PCR was performed and the results analyzed using an ABI PRISM 7000 sequence detection system (Applied Biosystems Inc., Foster City, CA). PCR was performed in a 20 μl volume reaction system containing 10 μl 2SYBR Green Reaction Mix (Invitrogen, Carlsbad, CA), 0.4 mmol/l paired primers, and 1 μl cDNA. Each sample was simultaneously run in triplicate. The sequences of the PCR primer pairs are listed in Table 1. Thermal cycling consisted of denaturation for 3 min at 95 °C, followed by 40 cycles of 15 s at 95 °C and 30 s at 60 °C. The PCR amplification efficiency of the primer sets was determined to be 100% before qPCR. A comparative Ct (ΔΔCt) method was used to compare the mRNA expression levels of the genes of interest. The glyceraldehyde-3-phosphate dehydrogenase (GAPDH) gene was chosen to be an internal control gene.

Western blot: The protein levels of HO-1 in the murine corneas were measured by western blots. Briefly, the corneas procured from the mice in the 100 μM group and the PBS group were homogenized in a 1.5 ml microtube with a lysis buffer (Beyotime Institute of Biotechnology, Shanghai, China) on day 4 after the alkali injury. Twenty-five corneas in each group were randomly divided and pooled into five samples, each of which had five corneas. Supernatants from each sample homogenate were collected after centrifugation at 24949 ×g for 30 min at 4 °C. Protein concentrations were quantified using a BCA Protein Assay Kit (Beyotime Institute of Biotechnology). Next, 20 μg of protein from each sample was mixed with a 2× sample buffer and heated to 100 °C for 5 min. After electrophoresis, the proteins were electrotransferred onto 0.2 mm PVDF membranes (Bio-Rad, Hercules, CA). The membranes were blocked with 5% skimmed milk and incubated overnight at 4 °C with primary antibodies (1:500, sc-10789, Santa Cruz Biotechnology). The staining specificity was assessed by the omission of the primary antibody. After three washes with tris-buffered saline (TBS), the membranes were incubated with a horseradish peroxidase-conjugated anti-rabbit IgG secondary antibody solution (1:1000, sc-2004, Santa Cruz Biotechnology) and then diluted in TBS with 5% skim milk for 2 h at room temperature. The membranes were then washed in TBS and placed in the chemiluminescent working solution (ECL detection reagents,

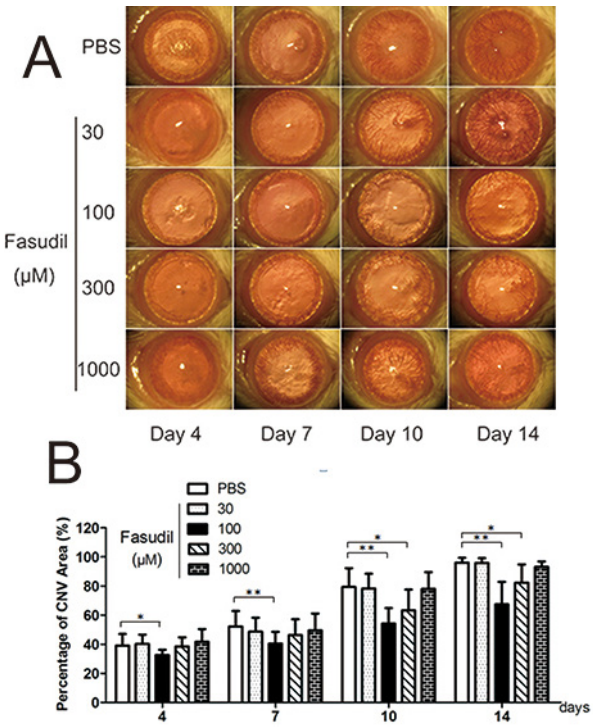

Figure 1. Inhibitory effect of fasudil eye drops on corneal neovascularization (CNV). **A**: Representative images of the murine corneas after alkali burns with and without fasudil eye drops. **B**: The percentages of CNV in the fasudil and phosphate-buffered saline (PBS) groups at every checkpoint. The percentages of CNV in the 30, 100, 300, and 1000 μM fasudil groups were 40.29%±6.30%, 32.54%±3.76%, 38.49%±6.27%, and 41.67%±8.78% on day 4; 48.61%±9.65%, 40.40%±8.15%, 46.36%±10.81%, and 49.52%±11.65% on day 7; 78.28%±10.21%, 54.17%±10.71%, 63.23%±14.32%, and 78.00%±11.57% on day 10; 95.89%±3.23%, 67.45%±15.45%, 82.38%±12.43%, and 93.16%±3.70% on day 14. The percentages of CNV in the PBS group were 39.04%±8.07%, 52.24%±10.58%, 79.34%±12.96%, 96.07%±3.32% on day 4, 7, 10, and 14, respectively (n=15/group, * indicates p<0.05, ** indicates p<0.01).

Thermo Fisher Scientific, Waltham, MA) for 5 min at room temperature. The membrane was imaged with a G:BOX BioImaging system (Syngene, Cambridge, England) at the same time, and the pictures were analyzed with Image J 1.62 software to measure the densitometric intensities of the respective bands. The experiment was repeated once.

Statistics: All data was expressed as mean ± standard deviation. The percentages of CNV and corneal epithelium defects were compared using one-way ANOVA between the four experimental groups and the control. A least-significant difference (LSD) analysis was performed to compare each experimental group and the control group. The expression levels of mRNAs, ROS production, and HO-1 proteins, as well as the number of infiltrated inflammatory cells, including PMNs, were compared using a Student *t* test for both the 100 μM fasudil group and the PBS group. A p value of less than 0.05 was considered to be statistically significant.

RESULTS

Effects of fasudil on alkali burn-induced CNV: The area of CNV was found to increase with time in both the experiment groups and the control group after alkali burns (Figure 1A). The percentages of CNV areas in the 100 μM fasudil treated group were significantly lower than those in the PBS treated group at every check point time (all p<0.05, Figure 1B). The percentages of CNV areas in the 300 μM fasudil treated group were lower than in the PBS treated group on days 10 and 14 (all p<0.05, Figure 1B). The areas of CNV in the 100 μM fasudil treated group were smaller than in the 300 μM fasudil treated group. There were no statistical differences in the percentages of CNV areas between either the 30 μM or the 1000 μM fasudil treated groups and the control group at any checkpoint after injury.

Fasudil promotes corneal epithelial healing: The percentages of corneal epithelial defect area to the entire cornea in the fasudil treated groups were lower than those in the PBS treated group on days 4 and 7 after the alkali burns (all p<0.01), with the exception of the 30 μM fasudil treated group on day 4. By day 10, the murine corneas had re-epithelialized in all groups (Figure 2).

The production of ROS in the cornea was enhanced after alkali burns and was then inhibited after treatment with 100 μM fasudil: To evaluate the effect of fasudil on ROS formation after the alkali burns, ROS production was examined using a DHE assay, in which DHE reacts with to show fluorescent imaging. The results show that the production of ROS in the corneal epithelium and stroma after an alkali injury without treatment was 2.29±0.21 and 2.0±0.20 times

that of ROS production in the normal cornea (all p<0.01, n=5/group, Figure 3). After treatment with 100 µM fasudil eye drops, the intensity of ROS-associated DHE fluorescence was significantly reduced in the corneal epithelium and stroma (all p<0.01, n=5/group, Figure 3).There was no statistical difference in the production of ROS between the mice with and without PBS treatment after injury, either in the corneal epithelium or in the stroma.

100 µM fasudil reduced the infiltration of inflammatory cells in the alkali-burned murine corneas: The histopathological analysis reveals a significant decrease in the number of infiltrated macrophages, lymphocytes, and PMNs in murine corneas after treatment with 100 µM fasudil eye drops compared to corneas treated with PBS (18.4±5.31 versus 47.8±9.01 per field, p<0.01; Figure 4A-C).The number of monoclonal antibody stained PMNs in the corneal stroma was significantly lower in the 100 µM fasudil treated group than in the PBS treated group (5.0±4.6 versus 16.0±5.0 per field, p<0.01; Figure 4D-F).

Effects of 100 µM fasudil on the mRNA expression of angiogenic genes in alkali-burned murine corneas: The mRNA expression levels of VEGF, VEGFR1/2, IL-1β, TNF-a, and MMP-2, MMP-8, and MMP-9 were detected and compared by quantitative RT-PCR. Gene expression was significantly lower in the 100 µM fasudil treated group; the expression levels were VEGF, 34.14%; TNF-α, 18.82%; MMP-8, 27.63%; and MMP-9, 12.57% compared to those in the PBS treated group. However, there were no statistical differences in the expression of VEGFR1/2, IL-1β, and MMP-2 between these two groups (Figure 5).

Effect of 100 µM fasudil on the expression of heme oxygenase-1 (HO-1) protein in the murine corneas after the alkali burn: To assess the effect of fasudil on HO-1 expression in the murine corneas, we examined the HO-1 protein on day 4 after the injury using western blotting. The results indicated that the optical intensity of HO-1 protein bands in the 100 µM fasudil treated group was 1.52±0.34 times that of HO-1 protein bands in the PBS treated group (p<0.05, Figure 6).

DISCUSSION

The results of this study show that fasudil can inhibit alkali burn-induced CNV. The potency of fasudil was also demonstrated by its inhibition of hypoxia-induced angiogenesis in pulmonary hypertension and tumors [20,21] and diabetes-induced microvascular damage in the retina [22]. In this study, we found 100 µM fasudil hydrochloride eye drops to be most effective in inhibiting CNV. This effect of fasudil was not dose-dependent and inhibited cancer cell proliferation in a concentration-dependent manner [23].

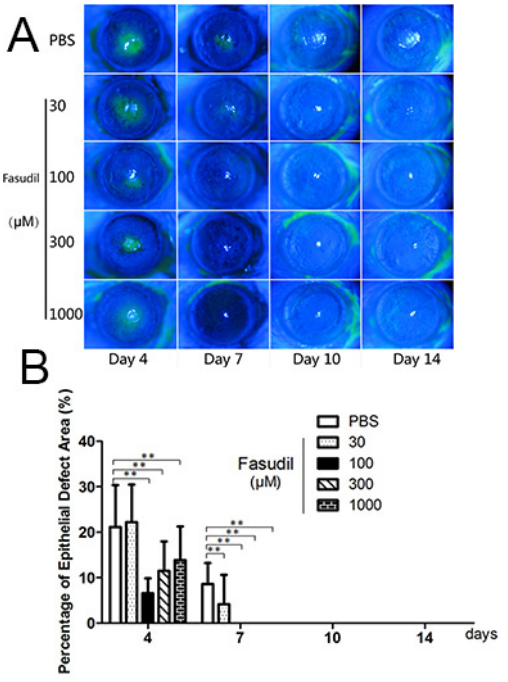

Figure 2. Fasudil promoted the healing of corneal epithelial defects after alkali burns. **A**: Representative images of the mice corneas with fluorescein staining after treatment with phosphate-buffered saline (PBS) or fasudil eye drops after alkali burns. **B**: The percentages of corneal epithelial defects were 22.21%±8.23%, 6.59%±3.27%, 11.50%±6.48%, and 13.90%±7.34% on day 4 and 4.20%±6.4%, 0%, 0%, and 0% on day 7 in the 30 µM, 100 µM, 300 µM, and 1000 µM fasudil groups. The corneal surfaces were re-epithelialized in all mice from day 10. So we don't need to compare the difference after day 10.The percentages of corneal epithelial defects were 21.15%±9.21% and 8.60%±4.60% in the PBS group on days 4 and 7, respectively (n=15/group, * indicates p<0.05, ** indicates p<0.01).

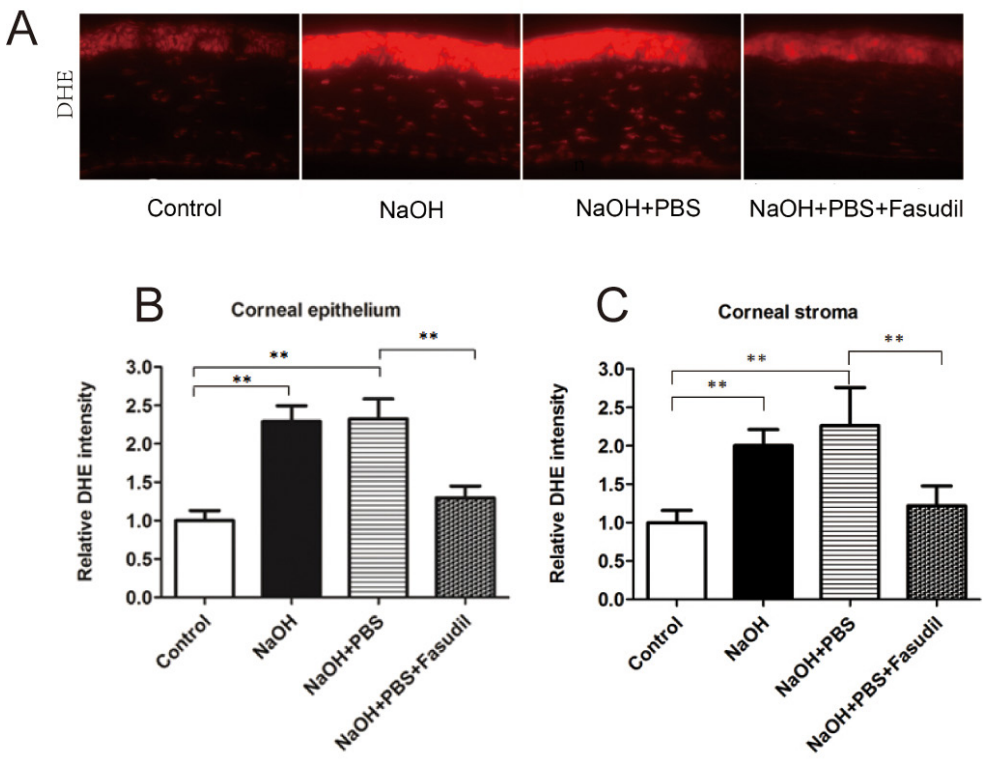

Figure 3. The production of reactive oxygen species (ROS) in the burned murine corneas with and without fasudil treatment. **A**: To evaluate the effect of fasudil on the production of ROS in the cornea after alkali burns using the dihydroethidium (DHE) assay, the intensity of fluorescence was scaled by integral optical density. **B**: In the corneal epithelium, the intensity of DHE fluorescence in the burned corneas after treatment with or without phosphate-buffered saline (PBS) was significantly higher than that in the normal corneas (503.9±56.7 and 496.8±44.9 versus 216.9±28.6, respectively; n=5/group, **p<0.01;), while it was significantly reduced after treatment with 100 μM fasudil eye drops (281.2±33.0; **p<0.01). **C**: In the corneal stroma, the intensity of DHE fluorescence in the burned corneas after treatment with or without PBS was significantly higher than that in the normal corneas (300.7±65.8 and 266.3±27.6 versus 132.9±21.1; n=5 per group, **p<0.01), while it was significantly reduced after treatment with 100μM fasudil eye drops (162±34.1; **p<0.01).

Inflammation is heavily involved in CNV, especially in chemical burn-induced CNV. After alkali burns, the inflammatory cells are recruited into the injured cornea, and some inflammatory cytokines are released. Following this, CNV will be induced, and the healing of corneal epithelial defects is delayed [24,25]. Most anti-inflammatory agents have shown a capacity to inhibit CNV, such as anti-VEGF agents [4,5], VEGF receptor inhibitors [26], anti-TNF-α agents [27], and anti-MMP agents [8]. The immunohistopathological results of this study show that the number of infiltrated inflammatory cells, including PMNs, in the murine cornea after alkali burns significantly decreased after the application of fasudil. Meanwhile, the mRNA expression of inflammatory cytokines, such as VEGF, TNF-α, MMP-8, and MMP-9, were downregulated. In previous reports, ROCK inhibition by fasudil could protect the vascular endothelium by inhibiting neutrophil adhesion and reducing neutrophil-induced endothelial injury in diabetic rats [22] and by decreasing the level of involved inflammatory cytokines, such as VEGF [28], TNF-α [29], MMP-2, and MMP-9 [30]. Our study further demonstrates the effectiveness of fasudil in reducing the infiltration of inflammatory cells, including PMNs, to the injured sites after which the associated inflammatory cytokines decrease in number. However, this study demonstrates that fasudil could not significantly reduce the mRNA expression of VEGFR1 and VEGFR2. Kubota et al. also demonstrated that fasudil had no effect on VEGFR2 and its phosphorylation in bovine retinal microvascular endothelial cells (BRECs) [10]. Furthermore, fasudil did not downregulate the mRNA expression of IL-1β and MMP-2 in this study, as it did in LPS-induced inflammation in endotoxemic mice [31] and in A549 lung cancer cells [23]. The mechanisms that contributed to this difference are still unknown.

Beyond inhibiting PMNs via the ROCK pathway, fasudil has been shown to reduce ROS production and potency after alkali burns in this study. The results of an ROS-related DHE fluorescence assay show that fasudil significantly reduced the production of ROS caused by alkali burns in the corneal epithelium and stroma. ROS formation in the cornea was enhanced immediately after alkali injury [10]. ROS, such as the superoxide radical (), hydrogen peroxide (), and the hydroxyl radical (), have been shown to be a driving force in the occurrence and development of CNV [10]. ROS can upregulate the expression of inflammatory cytokines (such as VEGF, interleukins, and TNF-α) via the nuclear factor-κB pathway [32,33] and promote the formation of CNV. Kubota et al. demonstrated that the application of antioxidant agents

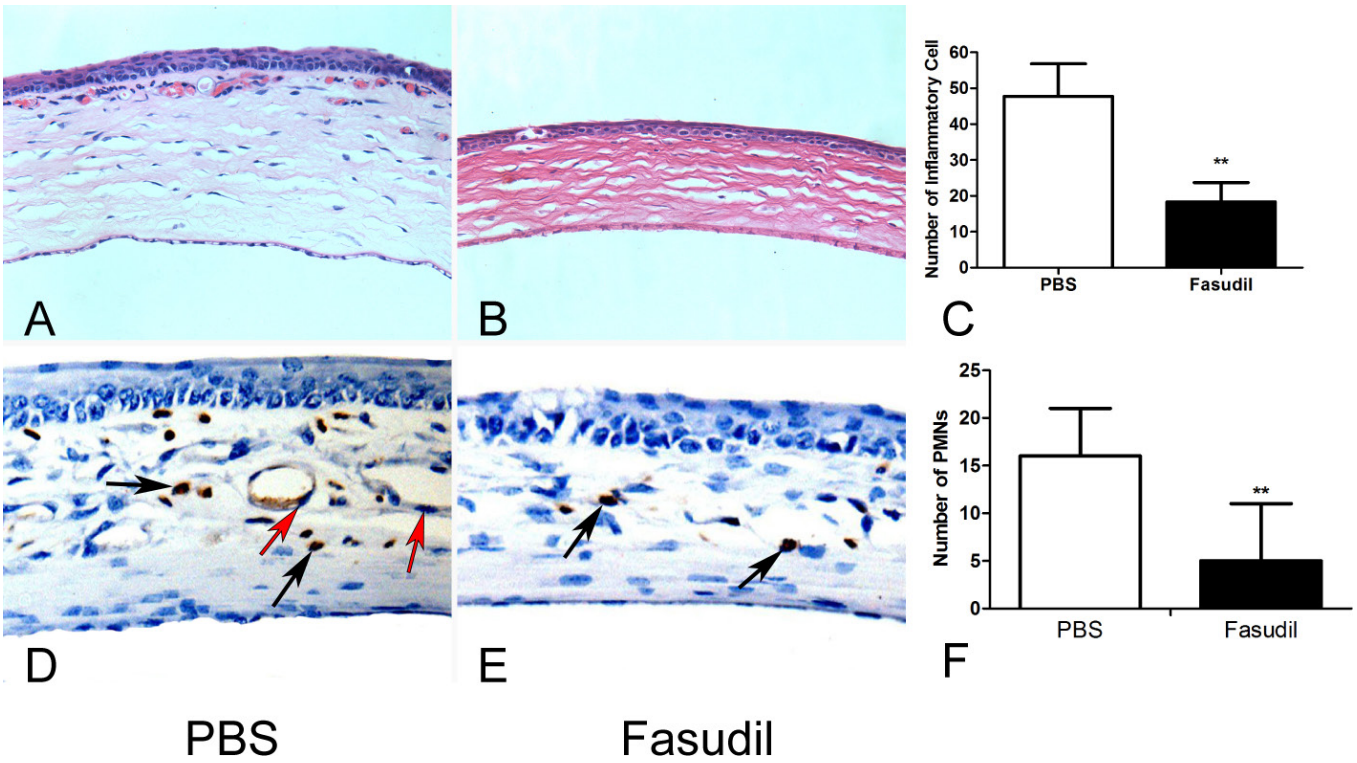

Figure 4. Anti-inflammatory effects of fasudil on the alkali-burned corneas. **A**–**C**: Hematoxylin-eosin staining of the murine corneas (magnification ×400). The number of infiltrated polymorphonuclear neutrophils (PMNs), macrophages, and lymphocytes in the corneal stroma per field was lower with 100 µM fasudil treatment than with phosphate-buffered saline (PBS) treatment. **D**–**F**: Immunohistochemical staining of PMNs. The endothelium of corneal vessels is indicated with red arrows. The number of infiltrated PMNs (brown staining, black arrows) in the corneal stroma per field was lower after100 µM fasudil treatment than with PBS treatment (n=7/group, ** indicates p<0.01).

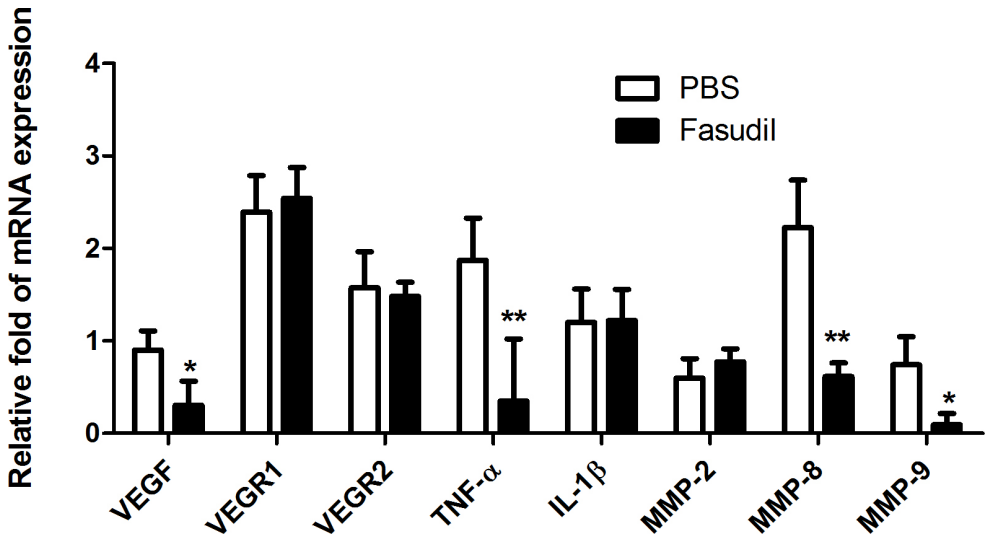

Figure 5. The mRNA expression of angiogenesis-related genes detected by real-time polymerase chain reaction (RT-PCR). All the data represented the relative fold change of mRNA expression of the genes of interest. There were statistically significant differences in the expression of VEGF, TNF-a, MMP-8, and MMP-9 between the 100 µM fasudil treated group and the phosphate-buffered saline (PBS) treated group (n=8/group, * indicates p<0.05, ** indicates p<0.01).

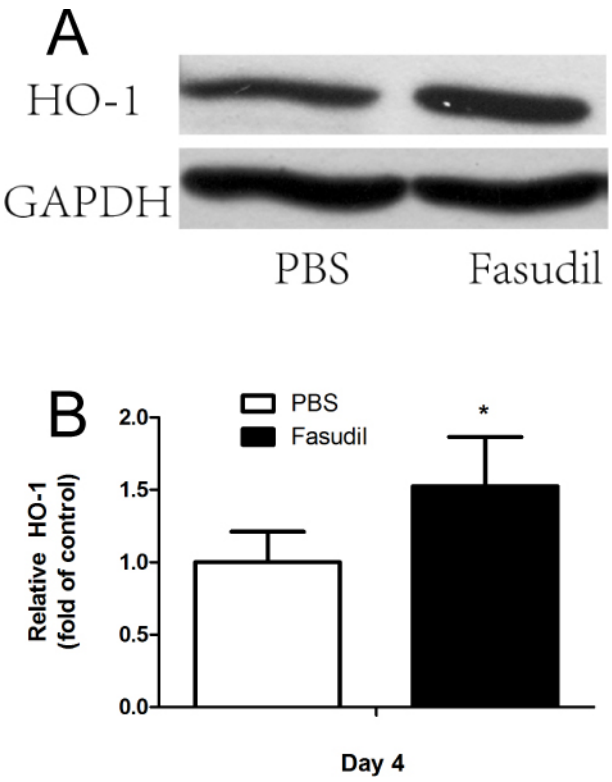

Figure 6. Effect of fasudil on the production of heme oxygenase-1 (HO-1) protein in the mice corneas after alkali burns. **A**: Representative image of western blotting bands for HO-1 protein in the murine corneas on day 4 after alkali burns. The intensity of fluorescence was scaled by integrated density. **B**: The protein expression of HO-1 after treatment with 100 µM fasudil eye drops was significantly enhanced compared to after phosphate-buffered saline (PBS) treatment (n=5 per group, * indicates $p<0.05$).

such as N-acetyl-L-cysteine for six consecutive days beginning from day 3 before the alkali burn can significantly reduce ROS production [10]. As an antioxidant agent, fasudil can reduce ROS production by inhibiting ROCK activation in vitro [15].

Furthermore, fasudil increased the expression of HO-1 protein after alkali burns in this study. HO-1 has been recognized as an important therapeutic target for cardiovascular diseases with high oxidative-stress levels, such as hypertension, diabetes, obesity, and myocardial ischemia-reperfusion injury [34-36]. The protective effect of increased HO-1 expression against endogenous ROS includes a reduction in cellular heme levels, the induction of ferritin, and the increased formation of bilirubin [37]. The evidence gathered shows that upregulation of HO-1 can not only reduce ROS levels in cells [38] but also prevent inflammation by inhibiting TLR pathway activation in vitro [39]. Thus, it is reasonable to assume that fasudil may suppress inflammation through the upregulation of HO-1 protein and the reduction of ROS formation via the Rho/ROCK pathway.

As a Rho-associated protein kinase (ROCK) inhibitor, fasudil promoted the healing of corneal epithelial defects after alkali burns in this study. Yin et al. also confirmed that Y-27632, a selective Rho-kinase inhibitor like fasudil, could accelerate the healing of corneal epithelial defects in wounded human corneal epithelial cells (HCECs) via the Rho/Rock pathway in vitro [40]. ROCK has been suggested to be involved in corneal epithelial differentiation [41], cell cycle progression [42], cell-cell adhesion [43], and cell-matrix interaction [44]. The inhibition of ROCK could enhance wound closure in cultured HCECs [40]. The promoted recovery of corneal wound healing may be attributed in part to the reduction of inflammatory cell infiltration and subsequent inhibition of CNV formation [45]. Our results were consistent with a previous report in which a specific ROCK inhibitor, Y-27632, could promote epithelial migration and attenuate cell proliferation. ROCK may play a negative role in regulating corneal epithelial wound healing. When negative regulation is inhibited, corneal wound healing may be promoted. However, another report showed that the acceleration of corneal epithelial migration activated by LPA (1-acyl-2-hydroxy-sn-glycero-3-phosphate) could be prevented by exoenzyme C3, a Rho inhibitor [46]. LPA acts at a cell surface receptor and stimulates corneal epithelial migration in an exoenzyme C3-sensitive manner through Rho. These conflicting results may be due to the different effects of Rho and ROCK inhibitors. The downstream effectors of Rho include ROCK, protein kinase N, rhotekin, citron, and mDia [47-51]. Theoretically, the activation of ROCK by LPA may inhibit epithelial migration. However, the other concurrent

activated downstream effectors like mDia may negate the effect of ROCK activation. A recent report suggested that mDia works concurrently with ROCKs. The Rho-induced actin reorganization and various actin fiber patterns rely on the balance between mDia and ROCK actions [50].

In summary, fasudil can inhibit the formation of CNV and accelerate the healing of corneal epithelial defects, as shown in this study. This may be attributed to the ability of fasudil to reduce the infiltration of inflammatory cells and the production of ROS as a potent ROCK inhibitor and its ability to increase HO-1 production to serve as an antioxidant. Further investigation is necessary to determine the pharmacodynamics, pharmacokinetics, safety, and tolerability of fasudil hydrochloride eye drops for ophthalmic application.

ACKNOWLEDGMENTS

Funding: supported in part by "Guangdong Scientific Program 2012" in China (Grant number: 2012B010300010).

REFERENCES

1. BenEzra D, Griffin BW, Maftzir G, Sharif NA, Clark AF. Topical formulations of novel angiostatic steroids inhibit rabbit corneal neovascularization. Invest Ophthalmol Vis Sci 1997; 38:1954-62. [PMID: 9331259].
2. Lee P, Wang CC, Adamis AP. Ocular neovascularization: an epidemiologic review. Surv Ophthalmol 1998; 43:245-69. [PMID: 9862312].
3. Chang JH, Gabison EE, Kato T, Azar DT. Corneal neovascularization. Curr Opin Ophthalmol 2001; 12:242-9. [PMID: 11507336].
4. Yoeruek E, Ziemssen F, Henke-Fahle S, Tatar O, Tura A, Grisanti S, Bartz-Schmidt KU, Szurman P. Safety, penetration and efficacy of topically applied bevacizumab: evaluation of eyedrops in corneal neovascularization after chemical burn. Acta Ophthalmol (Copenh) 2008; 86:322-8. [PMID: 17995975].
5. Papathanassiou M, Theodossiadis PG, Liarakos VS, Rouvas A, Giamarellos-Bourboulis EJ, Vergados IA. Inhibition of corneal neovascularization by subconjunctival bevacizumab in an animal model. Am J Ophthalmol 2008; 145:424-31. [PMID: 18207123].
6. Dana MR, Zhu SN, Yamada J. Topical modulation of interleukin-1 activity in corneal neovascularization. Cornea 1998; 17:403-9. [PMID: 9676913].
7. Saika S, Miyamoto T, Yamanaka O, Kato T, Ohnishi Y, Flanders KC, Ikeda K, Nakajima Y, Kao WW, Sato M, Muragaki Y, Ooshima A. Therapeutic effect of topical administration of SN50, an inhibitor of nuclear factor-kappaB, in treatment of corneal alkali burns in mice. Am J Pathol 2005; 166:1393-403. [PMID: 15855640].
8. Dan L, Shi-long Y, Miao-li L, Yong-ping L, Hong-jie M, Ying Z, Xiang-gui W. Inhibitory effect of oral doxycycline on neovascularization in a rat corneal alkali burn model of angiogenesis. Curr Eye Res 2008; 33:653-60. [PMID: 18696340].
9. Federici TJ. The non-antibiotic properties of tetracyclines: clinical potential in ophthalmic disease. Pharmacol Res 2011; 64:614-23. [PMID: 21843641].
10. Kubota M, Shimmura S, Kubota S, Miyashita H, Kato N, Noda K, Ozawa Y, Usui T, Ishida S, Umezawa K, Kurihara T, Tsubota K. Hydrogen and N-acetyl-L-cysteine rescue oxidative stress-induced angiogenesis in a mouse corneal alkali-burn model. Invest Ophthalmol Vis Sci 2011; 52:427-33. [PMID: 20847117].
11. Hoang MV, Whelan MC, Senger DR. Rho activity critically and selectively regulates endothelial cell organization during angiogenesis. Proc Natl Acad Sci USA 2004; 101:1874-9. [PMID: 14769914].
12. Hyvelin JM, Howell K, Nichol A, Costello CM, Preston RJ, McLoughlin P. Inhibition of Rho-kinase attenuates hypoxia-induced angiogenesis in the pulmonary circulation. Circ Res 2005; 97:185-91. [PMID: 15961717].
13. Iwasaki H, Okamoto R, Kato S, Konishi K, Mizutani H, Yamada N, Isaka N, Nakano T, Ito M. High glucose induces plasminogen activator inhibitor-1 expression through Rho/Rho-kinase-mediated NF-kappaB activation in bovine aortic endothelial cells. Atherosclerosis 2008; 196:22-8. [PMID: 17275007].
14. Bolick DT, Orr AW, Whetzel A, Srinivasan S, Hatley ME, Schwartz MA, Hedrick CC. 12/15-lipoxygenase regulates intercellular adhesion molecule-1 expression and monocyte adhesion to endothelium through activation of RhoA and nuclear factor-kappaB. Arterioscler Thromb Vasc Biol 2005; 25:2301-7. [PMID: 16166569].
15. Lu Y, Li H, Jian W, Zhuang J, Wang K, Peng W, Xu Y. The Rho/Rho-associated protein kinase inhibitor fasudil in the protection of endothelial cells against advanced glycation end products through the nuclear factor kappaB pathway. Exp Ther Med 2013; 6:310-6. [PMID: 24137180].
16. Asano T, Ikegaki I, Satoh S, Suzuki Y, Shibuya M, Takayasu M, Hidaka H. Mechanism of action of a novel antivasospasm drug, HA1077. J Pharmacol Exp Ther 1987; 241:1033-40. [PMID: 3598899].
17. Zhou SY, Xie ZL, Xiao O, Yang XR, Heng BC, Sato Y. Inhibition of mouse alkali burn induced-corneal neovascularization by recombinant adenovirus encoding human vasohibin-1. Mol Vis 2010; 16:1389-98. [PMID: 20680097].
18. Proia AD, Chandler DB, Haynes WL, Smith CF, Suvarnamani C, Erkel FH, Klintworth GK. Quantitation of corneal neovascularization using computerized image analysis. Lab Invest 1988; 58:473-9. [PMID: 2451768].
19. Berent-Spillson A, Russell JW. Metabotropic glutamate receptor 3 protects neurons from glucose-induced oxidative injury by increasing intracellular glutathione concentration. J Neurochem 2007; 101:342-54. [PMID: 17402968].

20. Abe K, Tawara S, Oi K, Hizume T, Uwatoku T, Fukumoto Y, Kaibuchi K, Shimokawa H. Long-term inhibition of Rho-kinase ameliorates hypoxia-induced pulmonary hypertension in mice. J Cardiovasc Pharmacol 2006; 48:280-5. [PMID: 17204906].

21. Takata K, Morishige K, Takahashi T, Hashimoto K, Tsutsumi S, Yin L, Ohta T, Kawagoe J, Takahashi K, Kurachi H. Fasudil-induced hypoxia-inducible factor-1alpha degradation disrupts a hypoxia-driven vascular endothelial growth factor autocrine mechanism in endothelial cells. Mol Cancer Ther 2008; 7:1551-61. [PMID: 18566226].

22. Arita R, Hata Y, Nakao S, Kita T, Miura M, Kawahara S, Zandi S, Almulki L, Tayyari F, Shimokawa H, Hafezi-Moghadam A, Ishibashi T. Rho kinase inhibition by fasudil ameliorates diabetes-induced microvascular damage. Diabetes 2009; 58:215-26. [PMID: 18840783].

23. Zhu F, Zhang Z, Wu G, Li Z, Zhang R, Ren J, Nong L. Rho kinase inhibitor fasudil suppresses migration and invasion though down-regulating the expression of VEGF in lung cancer cell line A549. Med Oncol 2011; 28:565-71. [PMID: 20300976].

24. Wagoner MD. Chemical injuries of the eye: current concepts in pathophysiology and therapy. Surv Ophthalmol 1997; 41:275-313. [PMID: 9104767].

25. Carter RT, Kambampati R, Murphy CJ, Bentley E. Expression of matrix metalloproteinase 2 and 9 in experimentally wounded canine corneas and spontaneous chronic corneal epithelial defects. Cornea 2007; 26:1213-9. [PMID: 18043179].

26. Mochimaru H, Usui T, Yaguchi T, Nagahama Y, Hasegawa G, Usui Y, Shimmura S, Tsubota K, Amano S, Kawakami Y, Ishida S. Suppression of alkali burn-induced corneal neovascularization by dendritic cell vaccination targeting VEGF receptor 2. Invest Ophthalmol Vis Sci 2008; 49:2172-7. [PMID: 18263815].

27. Cade F, Paschalis EI, Regatieri CV, Vavvas DG, Dana R, Dohlman CH. Alkali burn to the eye: protection using TNF-alpha inhibition. Cornea 2014; 33:382-9. [PMID: 24488127].

28. Celik F, Ulas F, Ozunal ZG, Firat T, Celebi S, Dogan U. Comparison of the effect of intravitreal bevacizumab and intravitreal fasudil on retinal VEGF, TNFalpha, and caspase 3 levels in an experimental diabetes model. Int J Ophthalmol 2014; 7:57-61. [PMID: 24634864].

29. Ma DW, Wang QY, Ma XY, Li J, Guan QH, Fu Y. The effect of fasudil via Rho/ROCK signaling pathway on the inflammation and fibrosis in human mesangial cells in high glucose medium. Zhonghua Nei Ke Za Zhi 2011; 50:580-4. [PMID: 22041269].

30. Yang X, Zhang Y, Wang S, Shi W. Effect of fasudil on growth, adhesion, invasion, and migration of 95D lung carcinoma cells in vitro. Can J Physiol Pharmacol 2010; 88:874-9. [PMID: 20921973].

31. Ding RY, Zhao DM, Zhang ZD, Guo RX, Ma XC. Pretreatment of Rho kinase inhibitor inhibits systemic inflammation and prevents endotoxin-induced acute lung injury in mice. J Surg Res 2011; 171:e209-14. [PMID: 21962807].

32. Finkel T, Holbrook NJ. Oxidants, oxidative stress and the biology of ageing. Nature 2000; 408:239-47. [PMID: 11089981].

33. Baldwin AS Jr. The NF-kappa B and I kappa B proteins: new discoveries and insights. Annu Rev Immunol 1996; 14:649-83. [PMID: 8717528].

34. Abraham NG, Kappas A. Pharmacological and clinical aspects of heme oxygenase. Pharmacol Rev 2008; 60:79-127. [PMID: 18323402].

35. Hosick PA, Stec DE. Heme oxygenase, a novel target for the treatment of hypertension and obesity? Am J Physiol Regul Integr Comp Physiol 2012; 302:R207-14. [PMID: 22071158].

36. Ryter SW, Alam J, Choi AM. Heme oxygenase-1/carbon monoxide: from basic science to therapeutic applications. Physiol Rev 2006; 86:583-650. [PMID: 16601269].

37. Khitan Z, Harsh M, Sodhi K, Shapiro JI, Abraham NG. HO-1 Upregulation Attenuates Adipocyte Dysfunction, Obesity, and Isoprostane Levels in Mice Fed High Fructose Diets. J Nutr Metab 2014; 2014:980547-[PMID: 25295182].

38. Dröge W. Free radicals in the physiological control of cell function. Physiol Rev 2002; 82:47-95. [PMID: 11773609].

39. Vivot K, Langlois A, Bietiger W, Dal S, Seyfritz E, Pinget M, Jeandidier N, Maillard E, Gies JP, Sigrist S. Pro-inflammatory and pro-oxidant status of pancreatic islet in vitro is controlled by TLR-4 and HO-1 pathways. PLoS ONE 2014; 9:e107656-[PMID: 25343247].

40. Yin J, Yu FS. Rho kinases regulate corneal epithelial wound healing. Am J Physiol Cell Physiol 2008; 295:C378-87. [PMID: 18495812].

41. SundarRaj N, Kinchington PR, Wessel H, Goldblatt B, Hassell J, Vergnes JP, Anderson SC. A Rho-associated protein kinase: differentially distributed in limbal and corneal epithelia. Invest Ophthalmol Vis Sci 1998; 39:1266-72. [PMID: 9620089].

42. Anderson SC, SundarRaj N. Regulation of a Rho-associated kinase expression during the corneal epithelial cell cycle. Invest Ophthalmol Vis Sci 2001; 42:933-40. [PMID: 11274069].

43. Anderson SC, Stone C, Tkach L, SundarRaj N. Rho and Rho-kinase (ROCK) signaling in adherens and gap junction assembly in corneal epithelium. Invest Ophthalmol Vis Sci 2002; 43:978-86. [PMID: 11923237].

44. Kim A, Lakshman N, Petroll WM. Quantitative assessment of local collagen matrix remodeling in 3-D culture: the role of Rho kinase. Exp Cell Res 2006; 312:3683-92. [PMID: 16978606].

45. Xiao O, Xie ZL, Lin BW, Yin XF, Pi RB, Zhou SY. Minocycline inhibits alkali burn-induced corneal neovascularization in mice. PLoS ONE 2012; 7:e41858-[PMID: 22848638].

46. Nakamura M, Nagano T, Chikama T, Nishida T. Role of the small GTP-binding protein rho in epithelial cell migration in

the rabbit cornea. Invest Ophthalmol Vis Sci 2001; 42:941-7. [PMID: 11274070].

47. Amano M, Mukai H, Ono Y, Chihara K, Matsui T, Hamajima Y, Okawa K, Iwamatsu A, Kaibuchi K. Identification of a putative target for Rho as the serine-threonine kinase protein kinase N. Science (New York, NY) 1996; 271:648-50. [PMID: 8571127].

48. Reid T, Furuyashiki T, Ishizaki T, Watanabe G, Watanabe N, Fujisawa K, Morii N, Madaule P, Narumiya S. Rhotekin, a new putative target for Rho bearing homology to a serine/threonine kinase, PKN, and rhophilin in the rho-binding domain. J Biol Chem 1996; 271:13556-60. [PMID: 8662891].

49. Madaule P, Eda M, Watanabe N, Fujisawa K, Matsuoka T, Bito H, Ishizaki T, Narumiya S. Role of citron kinase as a target of the small GTPase Rho in cytokinesis. Nature 1998; 394:491-4. [PMID: 9697773].

50. Watanabe N, Kato T, Fujita A, Ishizaki T, Narumiya S. Cooperation between mDia1 and ROCK in Rho-induced actin reorganization. Nat Cell Biol 1999; 1:136-43. [PMID: 10559899].

51. Matsui T, Amano M, Yamamoto T, Chihara K, Nakafuku M, Ito M, Nakano T, Okawa K, Iwamatsu A, Kaibuchi K. Rho-associated kinase, a novel serine/threonine kinase, as a putative target for small GTP binding protein Rho. EMBO J 1996; 15:2208-16. [PMID: 8641286].

Articles are provided courtesy of Emory University and the Zhongshan Ophthalmic Center, Sun Yat-sen University, P.R. China. The print version of this article was created on 12 June 2015. This reflects all typographical corrections and errata to the article through that date. Details of any changes may be found in the online version of the article.